Collective behavior in the single-electron charging regime through classical molecular dynamics

C. M. Carbonaro
Istituto Nazionale di Fisica della Materia, Dipartimento di Scienze Fisiche, Università degli Studi di Cagliari, Via Ospedale 72, I-09124 Cagliari, Italy

R. Bertoncini
Centro Richerche e Sviluppo, Studi Superiori in Sardegna, Casella Postale 1048, I-09123 Cagliari, Italy

F. Meloni
Istituto Nazionale di Fisica della Materia, D18-Dipartimento di Scienze Fisiche, Università degli Studi di Cagliari, Via Ospedale 72, I-09124 Cagliari, Italy

M. Rovere
Istituto Nazionale di Fisica della Materia, Dipartimento di Fisica, Università della Calabria, I-87036 Arcavacata di Rende, Italy

(Received 28 July 1995; revised manuscript received 28 November 1995)

We studied a semiconductor quantum wire having a smooth and continuous double-barrier potential superimposed along its length. The device is prepared at electron densities such that the interelectronic distance is bigger than the Bohr radius in GaAs. The strong Coulomb interaction between such carriers is accounted for exactly by classical molecular dynamics methods. We report the presence of charge-density-wave states as the main single-electron transport mechanism in this device.

I. INTRODUCTION

Mesoscopic devices with small capacitances have their operations dominated by charge-quantization phenomena whenever the charging energy associated with the addition of one electron into the structure exceeds the thermal energy.[1] These phenomena appear through periodic conductance oscillations as a function of carrier density, and are observed in devices such as metallic tunnel junctions,[2] silicon metal-oxide-semiconductor field-effect transistors[3] and GaAs/As$_x$Ga$_{1-x}$As heterojunctions.[4–6] Indeed, the possibility of exploiting these phenomena in the fabrication of high-frequency oscillators and low-power nonvolatile memories with improved endurance characteristics[7] and operating at 1 electron/bit (in contrast with the 10^4 or more of today's flash-EEPROM's) has spurred many experimental as well as theoretical efforts towards a better understanding of the physics underlying them.

In small metallic junctions, single-electron charging effects have been successfully explained, within the semiclassical Coulomb-blockade model, by invoking tunneling through the discrete energy levels of an electron in a quantum well, and accounting for the Coulomb interaction by the macroscopic device capacitance.[1]

In semiconductor structures, however, the various simplifications inherent in the Coulomb-blockade theory are no longer justified, and may lead to errors.[8] Unlike metallic systems, the potential barriers in semiconductor structures are, in general, smooth and continuous, and electron transfer may be activated thermically, through a continuous energy spectrum. This violates the basic requirement of the Coulomb-blockade formulation, for a discrete spectrum.

Furthermore, in a semiconductor device, the number of carriers can be controlled by changing the gate voltage.[9] At very low electron densities, as the screening length increases, additional effects in the transport properties are likely to appear because of the increased importance of the Coulomb interaction, which cannot, therefore, be accounted for by simple macroscopic-capacitance arguments. Indeed, below some critical density, an electron gas is expected to ''crystallize'' into a homogeneous ground state[10] whenever the Coulomb energy, which tends to localize electrons as far apart as possible from each other, dominates over the kinetic energy, which favors a smooth variation of the electron density. In semiconductor devices, therefore, as the interelectronic distance becomes comparable to, or even larger than, the device relevant lengths, increased stability charge-density waves (CDW) or Wigner crystal (WC) states are expected. Formation of CDW or WC has already been put forward to explain the periodic conductance oscillations in semiconductor devices.[4,5]

The purpose of this paper is to analyze the low-density regime by evaluating the microscopic electron-electron correlations exactly. As shown by several authors,[11–14] this can be accomplished by classical molecular dynamics simulations, which, by operating in the full classical regime, also allow one to account for the nontunneling transfer occurring with the smooth potential barriers present in semiconductor structures. Indeed, along the lines of Ref. 14, we consider single-electron charging phenomena in semiconductor devices to be a pure classical effect that can be activated thermically, and does not depend on the availability of a quantized spectrum. The formation of WC or CDW states relies on charge discreteness, and can be detected by classical nu-

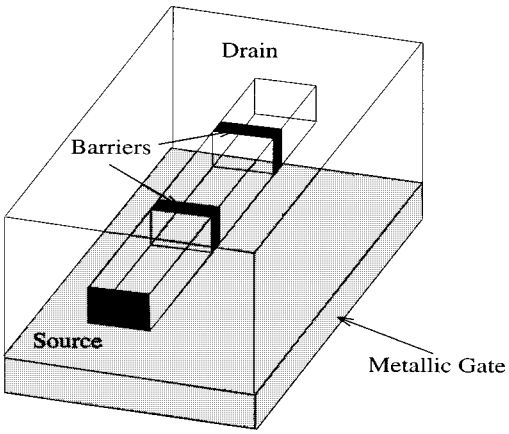

FIG. 1. Model structure of the wire and ground plane used in the simulation.

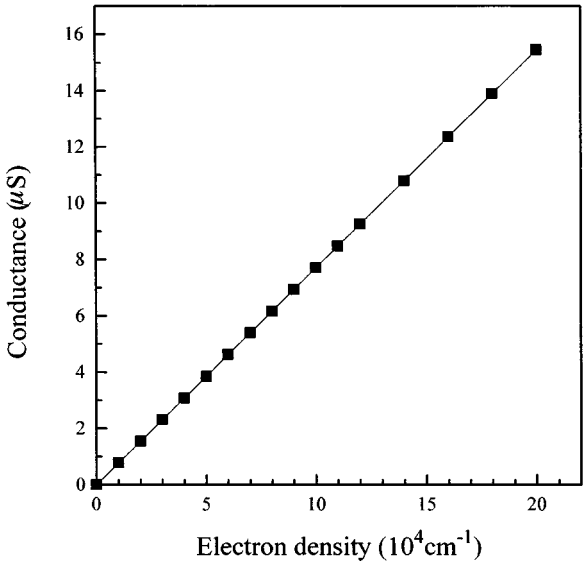

FIG. 2. Conductance vs electron density in the absence of potential barriers for a source-drain voltage of 425 μV at a temperature of 0.37 K. An electron density increment of 1.0×10^4 cm^{-1} corresponds to a gate voltage change of 0.475 mV (Ref. 18).

merical simulations provided a sufficiently low-density regime is considered, and the microscopic Coulomb interaction is properly taken into account.

This paper is organized as follows. In Sec. II we describe the physical model studied, and give full details of the setup for our numerical simulations. We do not, however, review the molecular dynamics methods as these can be found in a variety of textbooks.[15,16] In Sec. III the numerical results will be given, and a summarizing Sec. IV will conclude the paper.

II. PHYSICAL MODEL AND NUMERICAL METHOD

The device analyzed in this work is a semiconductor wire, such as obtained in a GaAs/Al_xGa_{1-x}As heterojunction transistors, with a superimposed double-barrier potential along its length.[5] This device allows for a direct control of its geometry, and observation of single-electron transport is achieved by simply applying a constant voltage.[17]

Our model consists of a classical one-dimensional electron gas with only one degree of freedom. This is justified since neither the shape of the confining potential determining the wire nor the structure of the transverse energy spectrum is relevant for the detection of charge-quantization phenomena. Only the Coulomb interaction is assumed, and an image charge is employed in order to mimic a positively charged metal gate that keeps electrical neutrality in the device. According to the experimental condition,[5,18] the image charge is placed at 0.725 μm away from the wire center.

The potential well is obtained from two Lorentzian-type barriers at a distance L_0. A schematic drawing of the device described is shown in Fig. 1. An applied source-drain voltage difference is considered by calculating the electric field force acting on the electrons in the device.

The classical equation of motion for the electron system is solved by the velocity-Verlet discretization algorithm. We adopted the usual periodic boundary conditions in order to avoid source-drain edge effects. The long-range tail of the Coulomb interaction is taken into account through the minimum image convention.[15]

The device contacts are dealt with by assuming that the electrons exiting the device equilibrate in the drain, losing all their velocity information. For each electron exiting the device, another must enter in order for the number of carriers to be conserved. The injected electron enters the device with its velocity assigned randomly according to a Maxwellian distribution that accounts for equilibration in the source contact.[19] Since this procedure is repeated several times during a simulation run, care must be taken in the choice of the random-number-generator and Gaussian-deviate routines, so as to assure a sufficiently long period and no sensible sequential correlation in the generation of the random numbers.[20]

The time step δt for the integration of Newton's equations was optimized so as to both ensure that the system energy is a constant for the motion (microcanonical ensemble), and to be able to cover the total simulation run with an acceptable CPU time. This leads to time steps of the order of 100 fs and simulation runs between 10 and 30 ns. We verified that the velocity change caused by the forces acting on the carriers is small, and the electron velocity is mainly due to the thermal energy, which, indeed, yields traversal times of the order of ns.

Once the time step was determined, the simulations were then performed in the canonical ensemble: the device is assumed to be in contact with a thermal bath and its temperature is kept constant by rescaling of the electrons' velocity.[15]

We evaluated the conductance as a function of the electron density n, which corresponds to variations of the gate voltage. Simulations in the classical regime are justified provided the average Coulomb interaction potential of the electronic system is larger then the Fermi level. This condition restricts the electron densities to a range where the interelectronic distances are larger than the Bohr radius a_B for the semiconductor material ($\sim$10 nm in GaAs). Therefore, we performed our simulations at densities up to 20×10^4 cm^{-1} where $na_B<0.5$. Under this condition, however, a one-dimensional Wigner crystal may form, and its pinning is expected whenever commensurability between its lattice con-

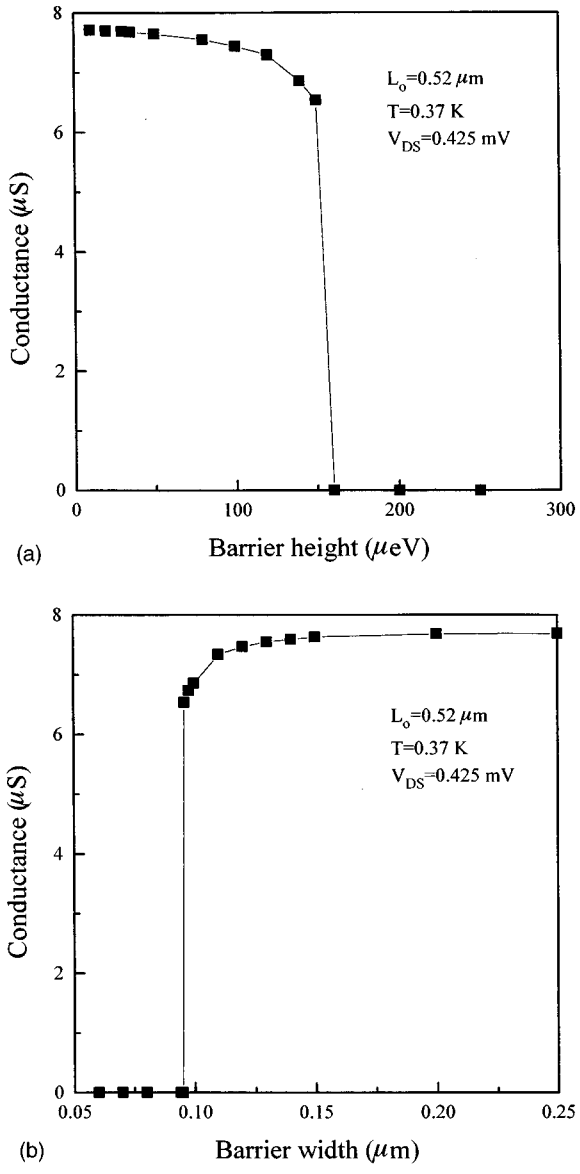

FIG. 3. Conductance dependence on the barrier height (a) and width (b).

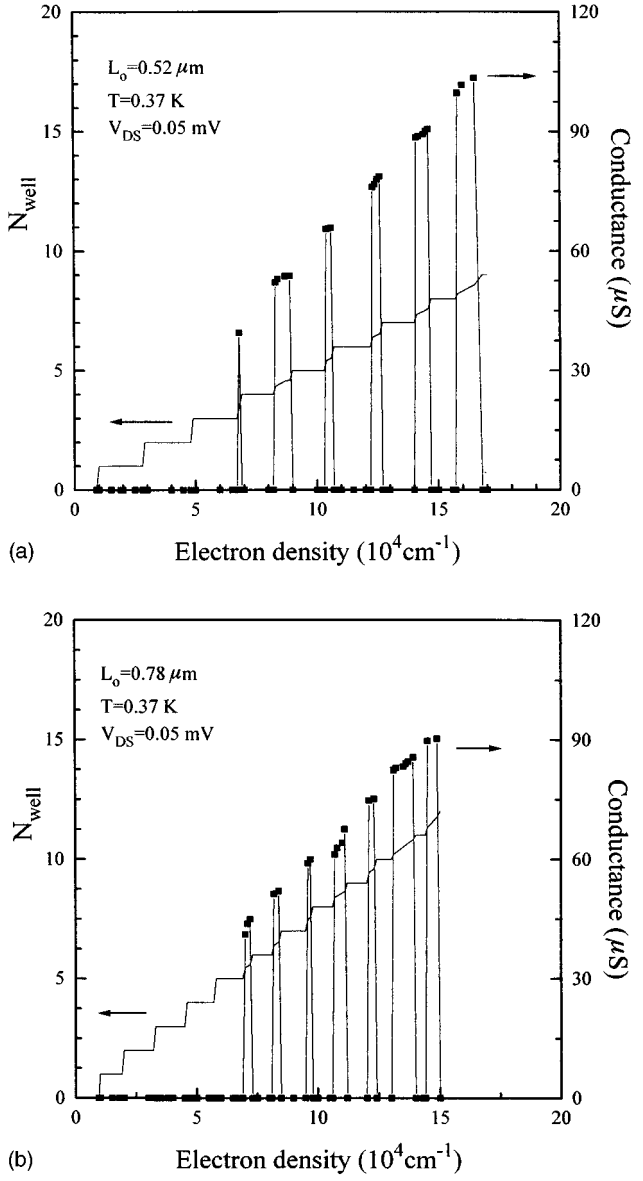

FIG. 4. Conductance vs electron density for two different values of the isolated segment L_0.

stant and the barriers distance L_0 is achieved.[4,21–23]

The different values for the electron density were obtained by varying both the number of electrons and the device length. In fact we need both a minimum number of electrons for the statistical average to be stable, and a device length bigger than the distance between the two barriers L_0. Therefore, we use a minimum device length of 1.0 μm and a minimum of ten electrons. On the other hand, we verified that the results obtained with a bigger number of particles do not differ significantly.

Conductance is given by the ratio between the applied voltage and the resulting current, which, in turn, is the charge variation in the unit time. Therefore, we evaluated the average time lapse between the passage of two electrons above the rightmost barrier. The choice of the point where the electron passage is detected is crucial: should electrons arrange themselves in a crystal-like configuration, they might oscillate, and carry no net current. Therefore, only if the electron detector is placed on a unsteady equilibrium point (a barrier peak), will no oscillating electron be recorded, and the net current at the drain is measured.

III. RESULTS

Before inserting the barriers in the device, we applied a source-drain bias of 0.425 mV and evaluated the wire conductance as a function of the carrier density. As shown in Fig. 2, the conductance has a linear behavior, as expected for an electron gas under the electric field drift force and the interparticle Coulomb interaction only.

In our simulation we noticed that once thermodynamical equilibrium is reached, all the particles assume equidistant positions, even when the initial system configuration is a random distribution of their coordinates: The lowest-energy configuration results in a crystal-like arrangement of the carriers. This indicates the predominant ''ordering'' role of the Coulomb force in our one-dimensional system.

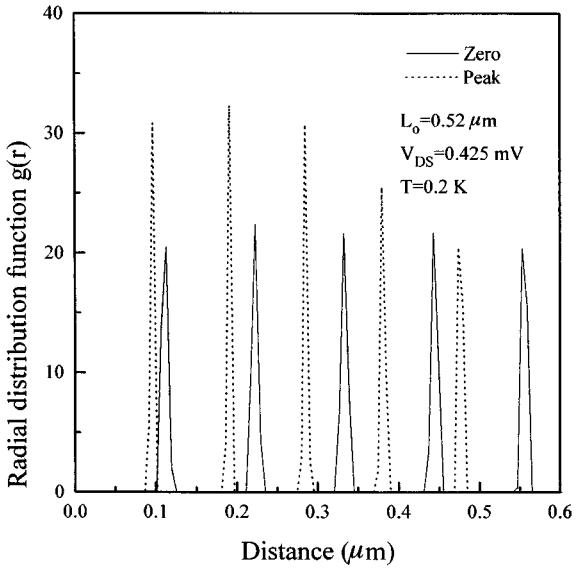

FIG. 5. Radial distribution function for a conductance zero and its adjacent peak.

The presence of the barriers in the device requires a detailed analysis, at a given carrier density, of the transport parameters with variation of the barrier dimensions. In Fig. 3, the conductance behavior at a density of 1×10^5 cm^{-1} for different barrier heights (h_b) and full widths at half height (w_b) is shown.

As expected for a system of classical particles, the conductance goes to zero discontinuously when h_b is increased beyond a threshold value corresponding to the electronic energy, whereas it saturates towards the ''unconstricted'' device as h_b is lowered.

An analogous discontinuity is present by increasing w_b, however this now accounts more directly for the discrete nature of the electrons: for small w_b the well is big enough for all of the electrons to be allocated inside it. No conduction can occur in this condition. Increasing w_b reduces the size of the well, and, thus, the number of electrons that can be trapped inside it. However, although the detrapping is now favored, and the conduction mechanism may yet be activated because of the discreteness of the charges, it cannot occur until the carriers' energy is high enough for the detrapping of at least one electron to occur.

Therefore, this analysis is crucial to the selection of the appropriate barrier parameters for the detection of the transport phenomena we are interested in. The choice of these parameters indeed lies in a limited range, further restricted by the fact that the extreme values should be discarded to avoid instabilities (at the discontinuity), or the unconstricted-device limiting case. An appropriate choice turned out to be $h_b=140$ μeV and $w_b=0.13$ μm.

In Fig. 4 the conductance for two different barrier distances L_0 is shown, together with a plot of the number of electrons $N_{\rm well}$ whose coordinates lie inside the well, between the barrier peaks. The conductance behavior is now highly nonlinear, with periodic peaks and zeros. Clearly, the zeros in the conductance correspond to an integer number of electrons being trapped into the potential well (plateau in the $N_{\rm well}$ curve), whereas the finite conductance values coincide

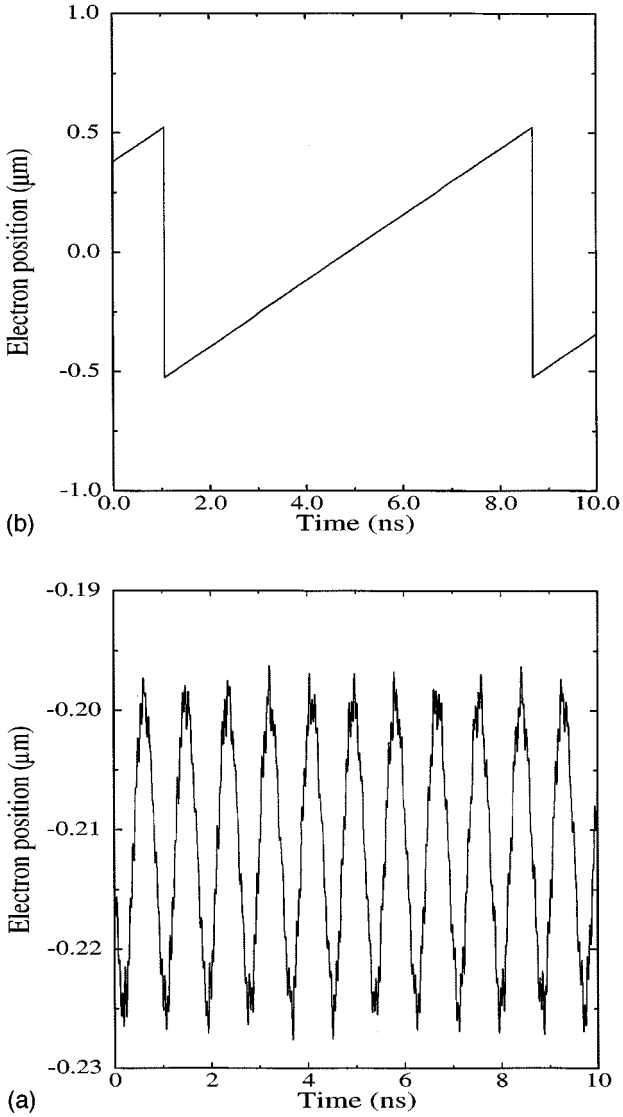

FIG. 6. Electron trajectories in the case of a conductance zero (a), and of the adjacent peak (b).

with the rise in $N_{\rm well}$. That the oscillations are related to the addition of a single electron to the isolated segment L_0 is confirmed by their period being inversely proportional to the barrier distance. As for the absolute values of the conductance, they are comparable with the experimental values, provided the temperature and the source-drain voltage V_{DS} are appropriately chosen, as we verified. Here, we prefer to show the results for a rather low V_{DS}, in order to have a sharper view of the single-electron charging.

During the simulation, we noticed that in correspondence to the conductance zeros, the average velocity of the electron system assumed alternating positive and negative values, the magnitude of which was smaller than in the case of any of the conductance peaks: all the electrons seem to oscillate around a fixed position.

In order to further investigate this phenomenon, we calculated the radial distribution function $g(r)$. This is shown in Fig. 5 for a conductance zero and its adjacent peak. In both cases, the system appears to have a crystalline structure, with all the electrons localized at their equilibrium positions,

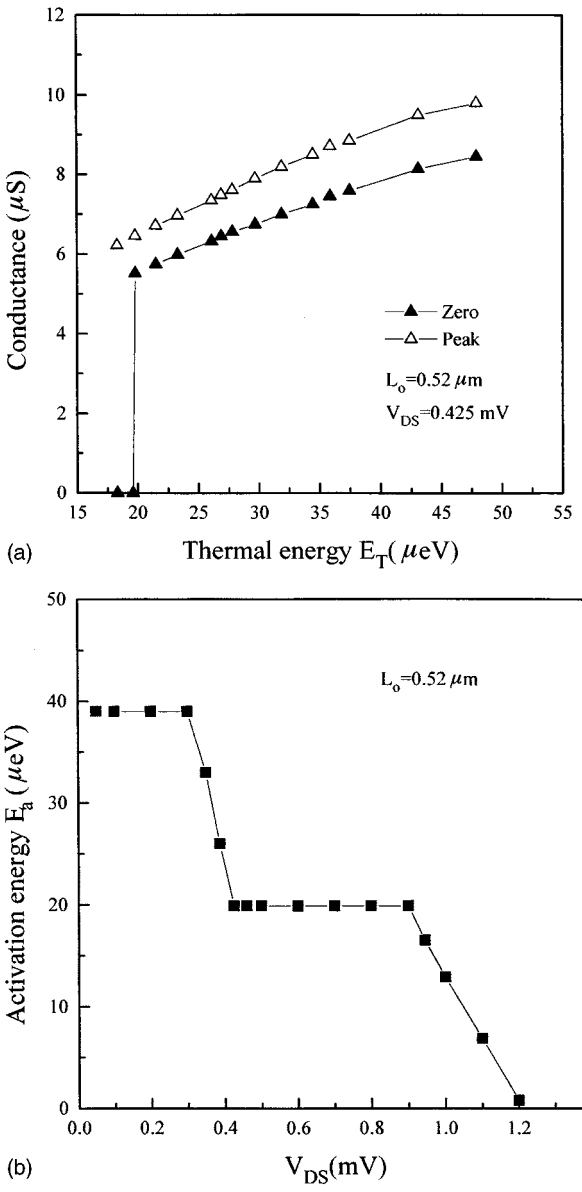

FIG. 7. (a) Temperature dependence of the conductance at a zero and a peak of an oscillation. (b) The dependence of the activation energy on the source-drain voltage.

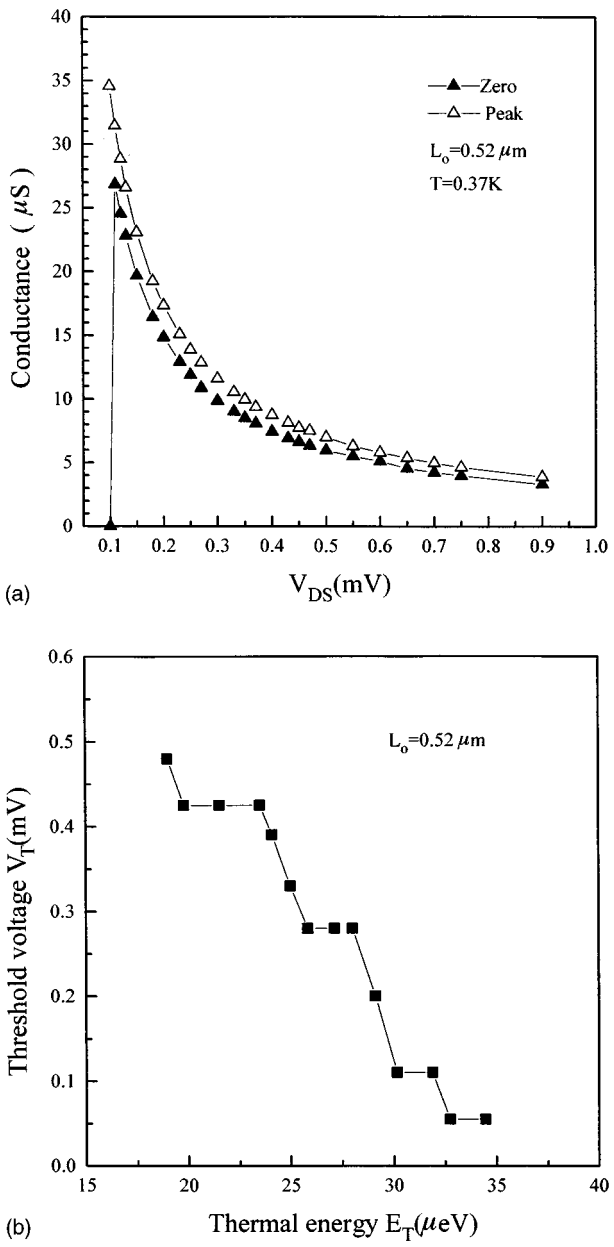

FIG. 8. (a) The dependence of the conductance on the source-drain voltage at a zero and a peak of an oscillation. (b) Temperature dependence of the threshold voltage.

the only difference being slightly wider peaks in the $g(r)$ from the case of the zero.

The conduction mechanism is, therefore, better explained through the analysis of the electron trajectories, as shown in Fig. 6. At the conductance zero, the whole system freezes, and the electrons oscillate around their positions (pinned CDW). For a finite value of the conductance, the system maintains its crystal structure, but now it slides as a whole along the device (sliding CDW). The periodic entering and leaving the device occurs at a frequency $f=I/e=1.44\times10^9$ s^{-1}, where I is the average dc current due to the electron motion.

The temperature dependence of the conductance is most clearly examined by plotting the conductance at one pair of the periodic peaks and zeros. This is done in Fig. 7(a): for a source-drain voltage of 0.425 mV, the conductance zero is characterized by a highly nonlinear behavior, with an activation energy of 0.198 μeV above which the oscillations disappear and the conductance assumes the value it would have in the absence of the barriers (Fig. 2).

We then analyzed the influence of finite source-drain voltage on the activation energy [Fig. 7(b)]. In the limit of very small V_{DS}, where the influence of the finite source-drain voltage can be excluded, the activation energy is found to be 39 μeV, quite close to the experimental value of Scott-Thomas *et al.*[3] The most striking feature, however, is the stepwise behavior of E_a. It means that there are stable electronic configurations that are not changed by the energy supplied by the electric field, and are, therefore, characterized by a constant activation energy. The total energy of the collective system of electrons has a bandlike structure, with energy gaps separated by ranges of continuous energy spectra, as

indicated by the linear step rises in Fig. 7(b).

For the same zero considered in the previous figure, the conductance dependence on the source-drain voltage [Fig. 8(a)] shows a threshold value, $V_T = 0.11$ mV at $T = 0.37$ K. <<<Beyond $V_T = 0.11$ mV the conductance rises by orders of magnitude, and then decreases at the same rates as for the peak, both values eventually approaching the ones they would have in the ''unconstricted case.'' The threshold voltage increases with a decrease in temperature, as shown in Fig. 8(b) where a stepwise structure can again be observed. This behavior confirms the band structure of the system total energy.

IV. CONCLUSIONS

We analyzed several types of potential barriers in order to verify which of them is more suitable for the observation of conductance oscillations, and whether the single-electron transfer is affected by their different shapes. We could not find any qualitative difference between the several barriers shapes studied.

It is difficult to devise a one-electron explanation for all these data, especially within the classical regime imposed by the molecular dynamics techniques employed here. A picture that explains our results is the one suggested by several authors[3,4,23] in which the electron in the device forms a charge-density wave or a Wigner crystal, as already mentioned above.

A pinned CDW is formed whenever the interelectronic distance is such as to allow precisely an integer number of particles to fit into the well, namely, when an integer number of periods of the density wave is commensurate with the isolated segment L_0. The whole system then freezes, and the conductance goes to zero, since the collective energy can be lowered without breaking the periodical arrangement of the electrons. Indeed, the radial distribution function shows a crystalline structure where, as clearly shown by the electron trajectories, each particle has an oscillatory motion.

Increasing the density, the interelectronic spacing is reduced to the extent that only a noninteger number of electrons could be trapped into the well. However, the discrete nature of the particles and the Coulomb force binding them do not allow a noninteger number of electrons to fall into the well. Thus, all the particles traverse the device, none getting trapped. The radial distribution function still shows a crystalline structure; however, now each particle does not have an oscillatory motion around its equilibrium position, but the whole system slides rigidly along the device, from source to drain. Therefore, as the density increases, the pinning strength oscillates and with it the conductance, which assumes a value of zero each time the commensurability condition is satisfied.[4]

Within this model, the bandlike structure of the collective energy spectrum, as it appears through the stepwise behavior of both the activation energy and the threshold voltage, indicates the existence of stable energy configurations that hold on within some range of temperature or of the applied voltage. The stable configurations are separated by unstable ones, where infinitesimal change of one of the parameters causes a corresponding change in the others. Such behavior further confirms the pinning and/or depinning of a particular CDW pattern by the segment L_0 as the main transport mechanism in this device.[24]

ACKNOWLEDGMENT

This work was supported by the Regione Autonoma della Sardegna.

[1] D. V. Averin and K. K. Lakharev, J. Low Temp. Phys. **62**, 345 (1986).
[2] T. A. Fulton and G. J. Dolan, Phys. Rev. Lett. **59**, 109 (1987).
[3] J. H. F. Scott-Thomas, S. B. Field, M. A. Kastner, H. I. Smith, and D. A. Antoniadis, Phys. Rev. Lett. **62**, 583 (1989).
[4] U. Meirav, M. A. Kastner, M. Heiblum, and S. J. Wind, Phys. Rev. B **40**, 5871 (1989).
[5] U. Meirav, M. A. Kastner, and S. J. Wind, Phys. Rev. Lett. **65**, 771 (1990).
[6] P. L. McEuen, E. B. Foxman, U. Meirav, M. A. Kastner, Y. Meir, N. Wingreen, and S. J. Wind, Phys. Rev. Lett. **66**, 1926 (1991).
[7] K. Yano, T. Ishii, T. Hashimoto, T. Kobayashi, F. Murai, and K. Seki, IEEE-IEDM 541 (1993).
[8] W. Häusler, B. Kramer, and J. Mašek, Z. Phys. B **85**, 435 (1991).
[9] See *Nanostructure Physics and Fabrication*, edited by M. Reed and W. P. Kirk (Academic, New York, 1989).
[10] E. Wigner, Phys. Rev. **46**, 1002 (1934).
[11] P. Lugli and D. K. Ferry, Phys. Rev. Lett. **56**, 1295 (1986).
[12] P. Lugli, C. Jacoboni, L. Reggiani, and P. Kocevar, Appl. Phys. Lett. **50**, 1251 (1987).
[13] M. J. Kann, A. M. Kriman, and D. K. Ferry, Phys. Rev. B **41**, 12 659 (1990).
[14] K. Yano, and D. K. Ferry, Phys. Rev. B **46**, 3865 (1992).
[15] M. P. Allen and D. J. Tildesley, *Computer Simulation of Liquids* (Clarendon, Oxford, 1991).
[16] R. W. Hockney and J. W. Eastwood, *Computer Simulation Using Particles* (Adam Hilger, Bristol, 1989).
[17] M. A. Kastner, Phys. Today **46**, 24 (1993).
[18] U. Meriav, M. Heiblum, and F. Stern, Appl. Phys. Lett. **52**, 1268 (1988).
[19] C. Jacoboni and P. Lugli, *The Monte Carlo Method for Semiconductor Device Simulation* (Springer-Verlag, Wien, 1989).
[20] W. H. Press, B. P. Flannery, S. A. Teukolsky, and W. T. Vetterling, *Numerical Recipes* (Cambridge University Press, Cambridge, 1990). IOP Conf. Proc. No. 43 (Institute of Physics and Physical Society, Bristol, 1979), p. 593.
[21] H. J. Schulz, J. Phys. Soc. Jpn. **49**, 861 (1980).
[22] L. I. Glazman, I. M. Ruzin, and B. I. Shklovski, Phys. Rev. B **45**, 8454 (1992).
[23] N. S. Bakhvalov, G. S. Kazacha, K. K. Likharev, and S. I. Serdyukova, IEEE Trans. Magn. **25**, 1436 (1989).